

Electronic Supplementary Information

Metal-organic frameworks derived yolk-shell NiS₂/carbon spheres for lithium-sulfur batteries with enhanced polysulfide redox kinetics

Yaxi Tian, Huawen Huang, Guoxue Liu, Ran Bi, and Lei Zhang*

School of Chemistry & Chemical Engineering, South China University of Technology,
Guangzhou 510640, P. R. China

E-mail:

celeizhang@scut.edu.cn

Experimental Section

Materials Synthesis

Synthesis of yolk-shell Ni-MOFs.

Yolk-shell Ni-MOFs was synthesized *via* a solvothermal method.^{S1} Typically, 0.15 g of trimesic acid, 1.5 g of polyvinylpyrrolidone (Sigma-Aldrich, Mw = 40,000), and 0.432 g of Ni(NO₃)₂·6H₂O were added to a mixture of 10 mL of H₂O, 10 mL of DMF, and 10 mL of ethanol to obtain a light green solution. After stirring for 40 min, the solution was then transferred to 50 mL of Teflon-line sealed autoclave and kept at 150 °C for 10 h. After cooling down to room temperature, the obtained light green product was collected by centrifugation and washed with ethanol for three times. For the synthesis of hollow Ni-MOFs, the hydrothermal time was prolonged to 15 h while the other condition is the same.

Synthesis of yolk-shell NiS₂/C.

0.1 g of yolk-shell Ni-MOFs and 0.08 g of sulfur powder were placed into a porcelain boat, where sulfur powder was placed at the upstream side of tube furnace. Then, the tube furnace was heated to 450 °C for 2 h with a ramp rate of 1 °C min⁻¹ in N₂ (60 mL min⁻¹). After cooling down to room temperature, the dark product was named as yolk-shell NiS₂/C. The hollow NiS₂/C spheres were formed by replacing yolk-shell Ni-MOFs spheres with hollow Ni-MOFs.

Synthesis of yolk-shell C.

0.1 g of yolk-shell Ni-MOFs was heated at 450 °C for 2 h with a ramp rate of 1 °C

min⁻¹ in N₂ (60 mL min⁻¹). After cooling down to room temperature, the dark product was added into 30 mL 2 M HCl, and heated at 150 °C for 24 h. The obtained product was washed with deionized water and ethanol for several times and dried at 60 °C.

Synthesis of yolk-shell NiS₂/C-S.

A mixture of yolk-shell NiS₂/C and sulfur powder with a mass ration of 3:7 was grinded for 30 min. Then, the mixture was transferred to 50 mL of Teflon-line sealed autoclave and heated at 155 °C for 24 h. After cooling down to temperature, yolk-shell NiS₂/C-S was obtained. For comparison, hollow NiS₂/C-S and yolk-shell C-S were prepared under the same condition.

Adsorption Experiments

Li₂S₆ solution was prepared by mixing Li₂S and sulfur with a molar ration of 1:5 in 1, 2-dimethoxyethane (DME), and stirred for 20 h at room temperature in an argon-filled glove box. 15 mg of yolk-shell C, hollow NiS₂/C and yolk-shell NiS₂/C were dispersed into 2.0 mL of Li₂S₆ solution and vigorously stirred to evaluate the adsorption capacity for Li₂S₆, respectively. The suspensions were centrifuged before photographs were taken.

Materials Characterizations

All the samples were characterized by field-emission scanning electron microscopy (FESEM; Hitachi SU8220), transmission electron microscopy (TEM; JEOL JEM-2100F), and X-ray diffraction (XRD; Bruker D8 Advance). Thermogravimetric analysis (TGA) was measured on the STA449 instrument with a ramp rate of 10 °C

min⁻¹ under a nitrogen atmosphere. The nitrogen sorption isotherms were measured on a Micromeritics 3 Flex system at liquid-nitrogen temperature.

Electrochemical Measurement

The working electrode was prepared by mixing active materials, conductive carbon, and poly(vinylidene fluoride) (PVDF) with a mass ration of 7:2:1 in N-methyl-2-pyrrolidinone (NMP) to make a homogenous slurry. The slurry was coated on the surface of carbon coated aluminum foil with the sulfur loading mass about 1.0 mg cm⁻². The electrolyte was 1.0 M Lithium bis(trifluoromethanesulfonyl)imide (LiTFSI) dissolved in dimethoxymethane/ 1,3-dioxolane (DME/DOL, 1:1, v/v) with 2.0 wt% LiNO₃. The amount of electrolyte is 20 μL mg⁻¹. Lithium metal foil and Celgard 2400 were used as the anode and separator, respectively. Galvanostatic charge/discharge tests were carried out using Neware Battery Testing System between 1.7 and 2.8 V. Cyclic voltammetry measurements were performed at a scan rate of 0.1 mV s⁻¹.

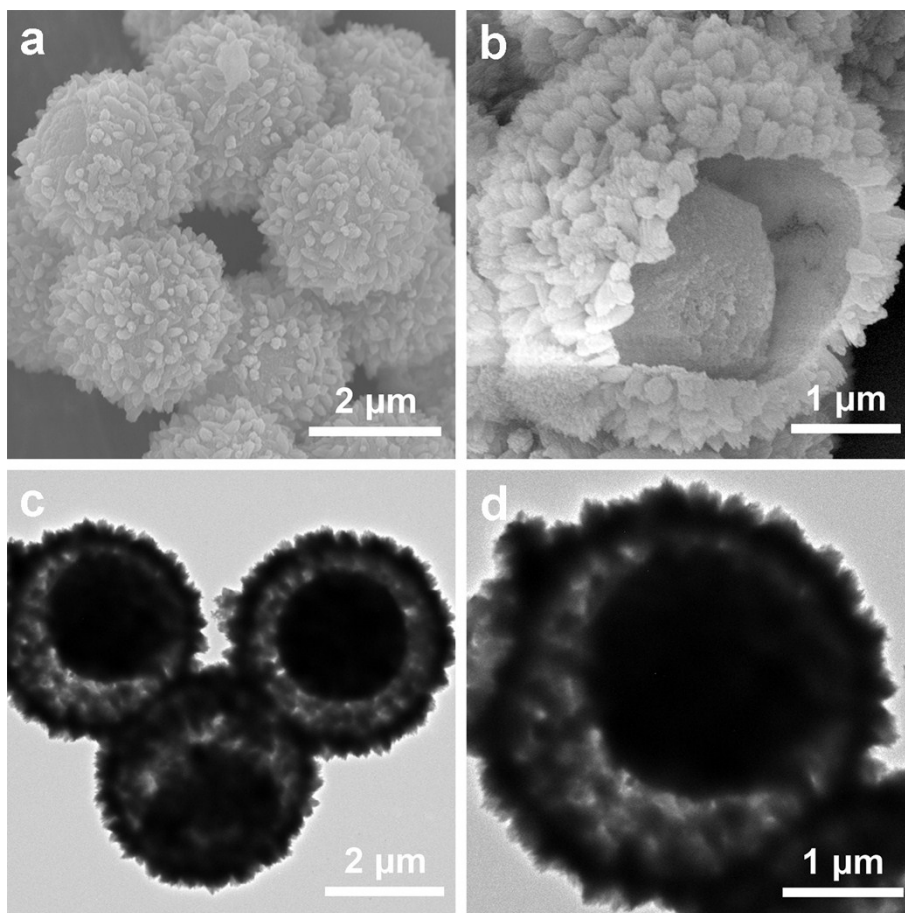


Fig. S1 (a, b) SEM and (c, d) TEM images of yolk-shell Ni-MOFs.

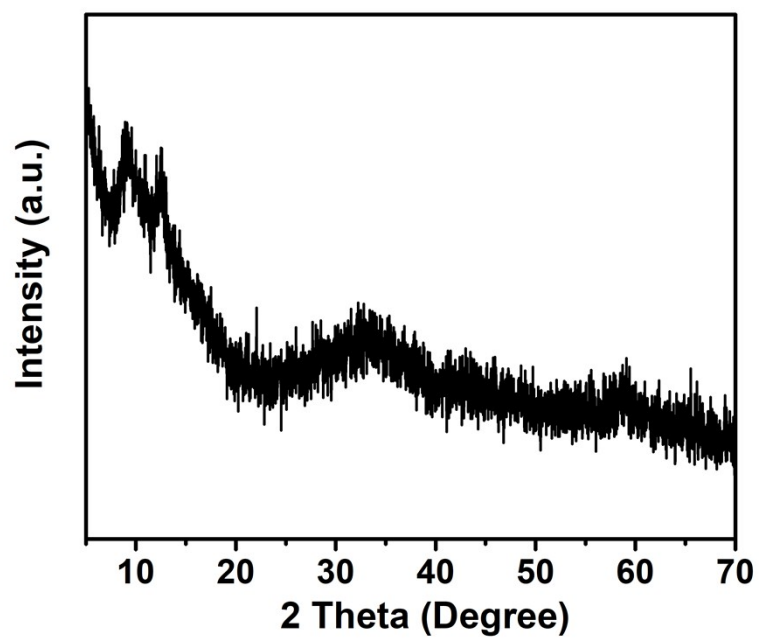


Fig. S2 XRD pattern of yolk-shell Ni-MOFs.

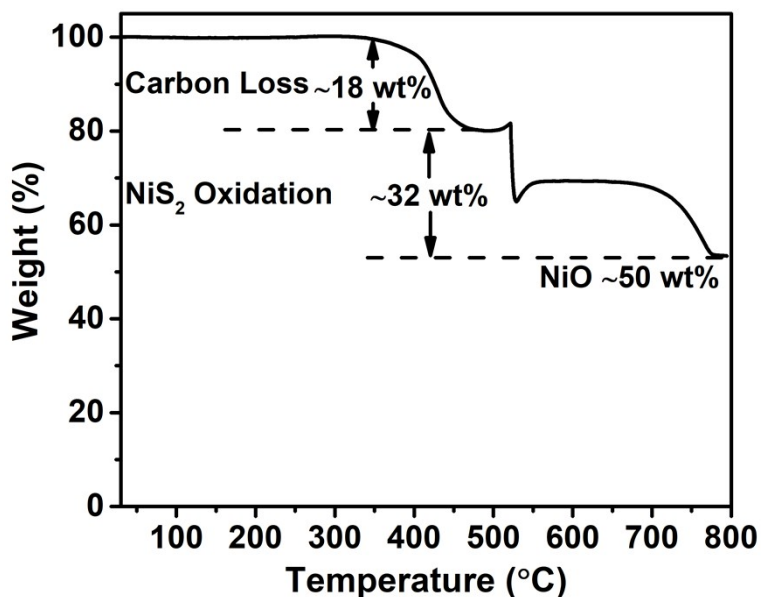
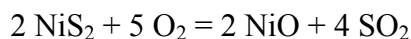


Fig. S3 Thermogravimetric analysis (TGA) curve of yolk-shell NiS₂/C in air with a heating rate of 10 °C min⁻¹.

The weight loss of 18 wt% between 300 and 450 °C is ascribed to the carbon loss. With the increasing temperature, NiS₂ is oxidized to NiS, NiO, and NiSO₄. The weight increase appearing 520 – 600 °C is observed owing to the formation of NiSO₄. The final residue is 50 wt% NiO. Based on the following chemical reaction:



the weight content of NiS₂ is calculated as follow:

$$\text{NiS}_2 \text{ wt\%} = 50 \text{ wt\%} \times \text{Mw}(\text{NiS}_2) \div \text{Mw}(\text{NiO}) = 50 \text{ wt\%} \times 123 \div 75 = 82 \text{ wt\%}.$$

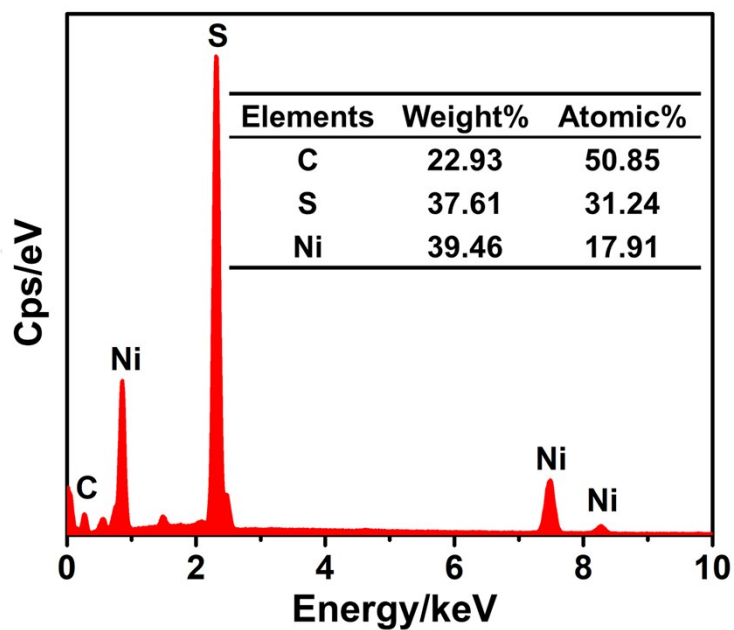


Fig. S4 Energy dispersive spectrometer in scanning electron microscopy (SEM-EDS) spectrum of yolk-shell NiS₂/C.

SEM-EDS spectrum result of yolk-shell NiS₂/C reveals that the atomic ratio of Ni and S is about 1:2. Based on the weight of Ni (39.46 wt%) and S (37.61 wt%) elements, the content of NiS₂ in the yolk-shell NiS₂/C is calculated as about 77 wt% (39.46 wt% + 37.61 wt%), which is very close to the result of TGA (**Fig. S3**).

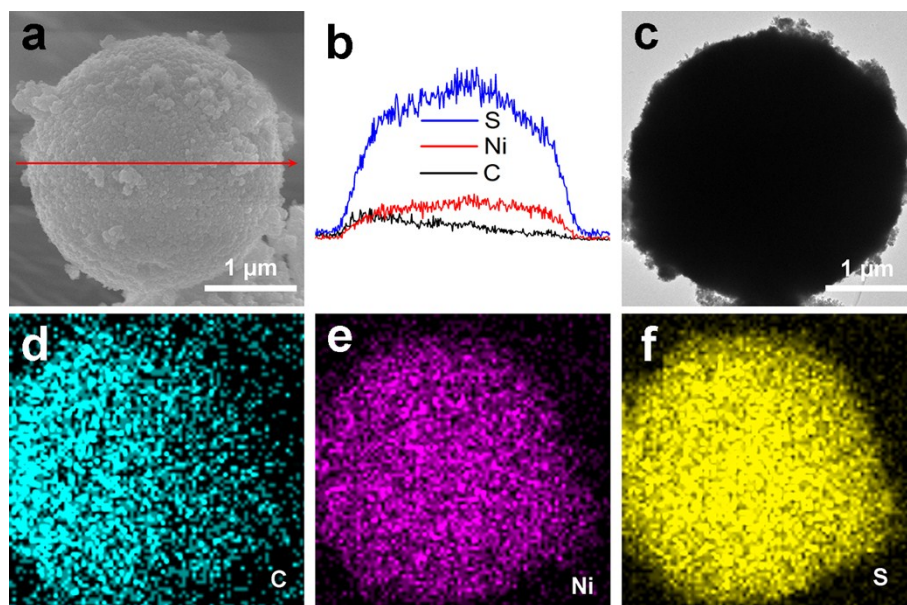


Fig. S5 (a) SEM image of yolk-shell $\text{NiS}_2/\text{C-S}$. (b) The line-scanning curves of C, Ni and S, corresponding to the red arrow in (a). (c) TEM image of yolk-shell $\text{NiS}_2/\text{C-S}$. (d–f) Element mapping of yolk-shell $\text{NiS}_2/\text{C-S}$.

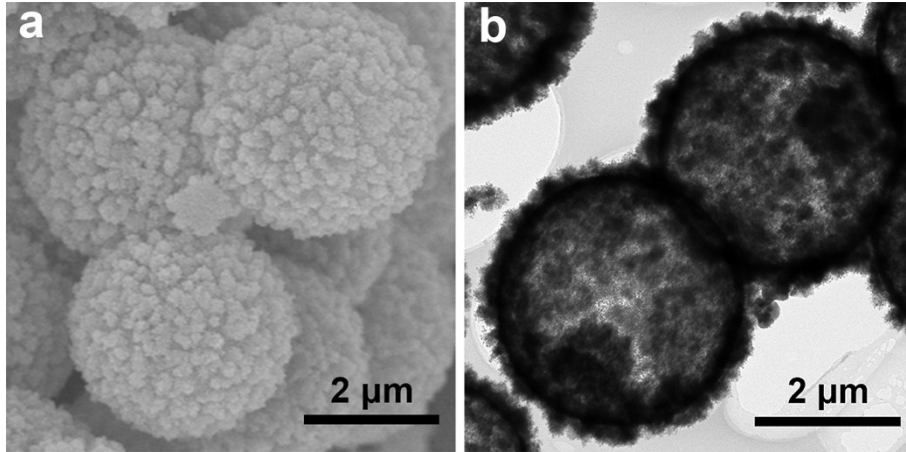


Fig. S6 (a) SEM and (b) TEM images of hollow NiS_2/C .

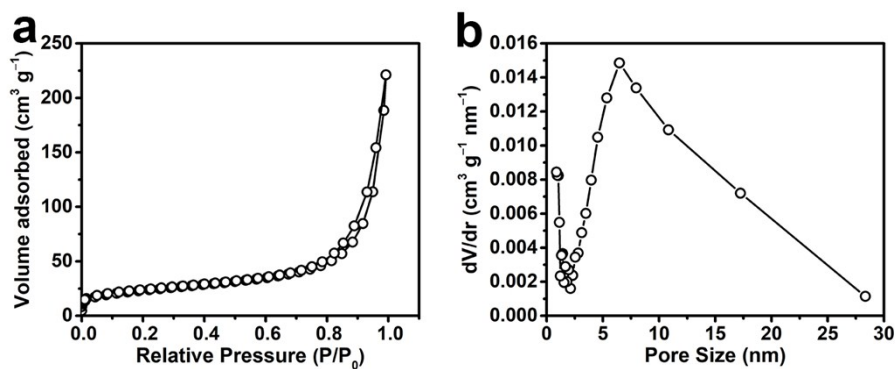


Fig. S7 (a) N₂ adsorption-desorption isotherm and (b) pore size distribution plot of hollow NiS₂/C.

The Brunauer-Emmett-Teller (BET) specific surface area of hollow NiS₂/C is investigated by the N₂ adsorption-desorption measurements. N₂ adsorption-desorption isotherm is IV type and pore size distribution is centred at 5–12 nm. The BET specific surface area of hollow NiS₂/C is 80.8 m² g⁻¹ (**Fig. S7**), which is very close to that of yolk-shell NiS₂/C (78.9 m² g⁻¹, **Fig. 3b**).

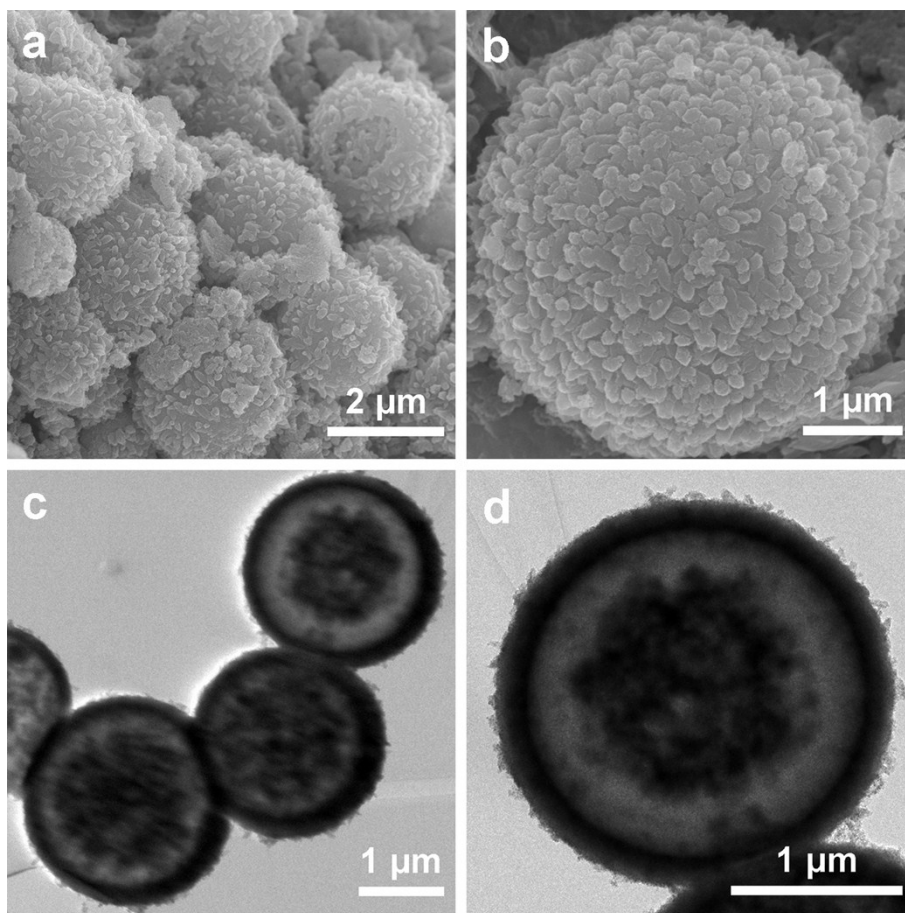


Fig. S8 (a, b) SEM and (c, d) TEM images of yolk-shell C.

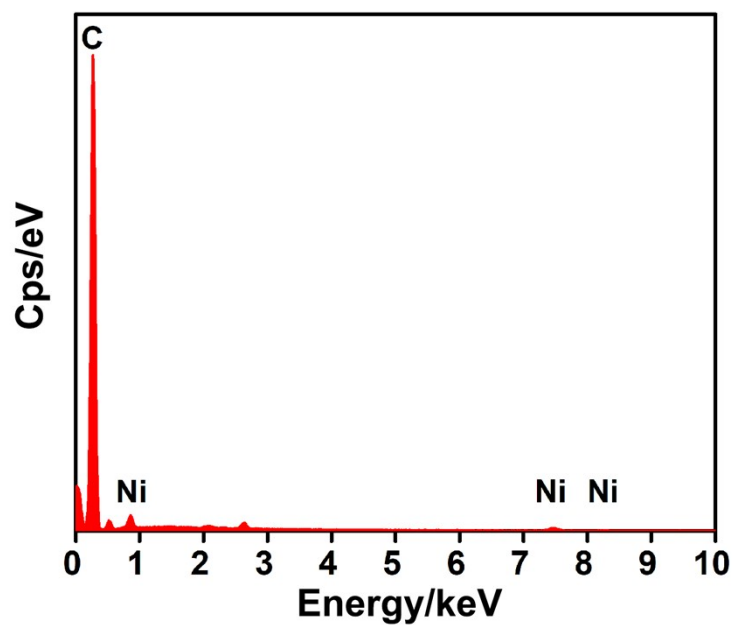


Fig. S9 Energy dispersive spectrometer in scanning electron microscopy (SEM-EDS) spectrum of yolk-shell C. The SEM-EDS spectrum result of yolk-shell C reveals that the Ni in the yolk-shell C has been removed.

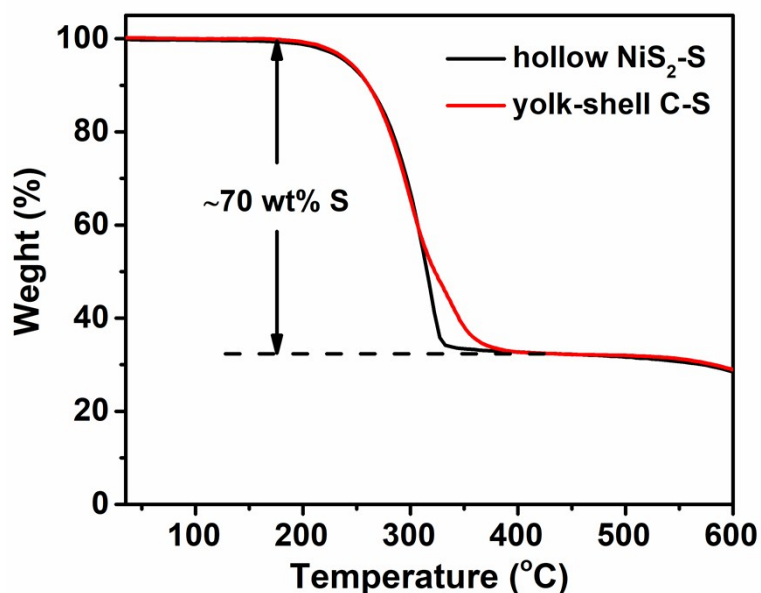


Fig. S10 TGA curves of hollow NiS₂/C-S and yolk-shell C-S in nitrogen with a heating rate of 10 °C min⁻¹.

TGA results reveal that the loading amount of sulfur in the hollow NiS₂/C-S and yolk-shell C-S both are about 70 wt% (**Fig. S10**), which are the same as that of yolk-shell NiS₂/C-S (**Fig. 3d**). Yolk-shell NiS₂/C-S, hollow NiS₂/C-S, and yolk-shell C-S cathodes has the similar loading amount of sulfur. When tested as sulfur cathodes, the different electrochemical performance of is yolk-shell NiS₂/C-S, hollow NiS₂/C-S, and yolk-shell C-S cathodes is mainly attributed to their different structure.

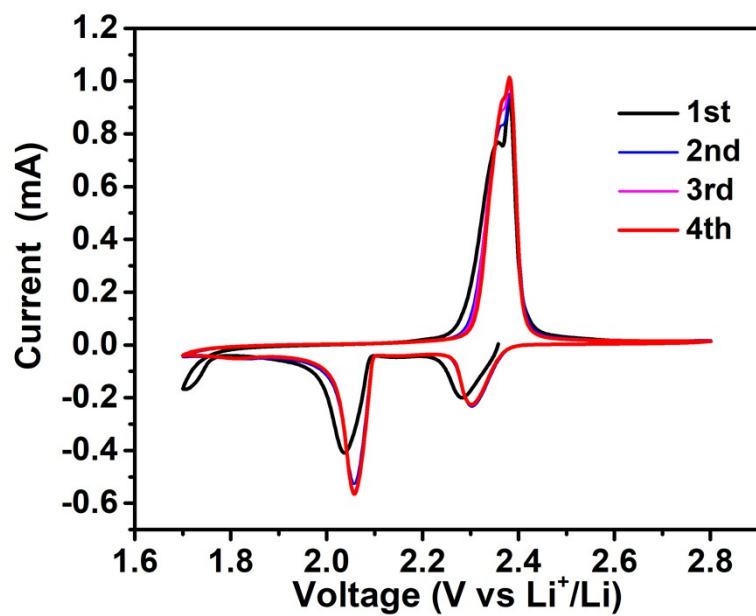


Fig. S11 Cyclic voltammograms curves of yolk-shell NiS₂/C-S cathode at a scan rate of 0.1 mV s⁻¹.

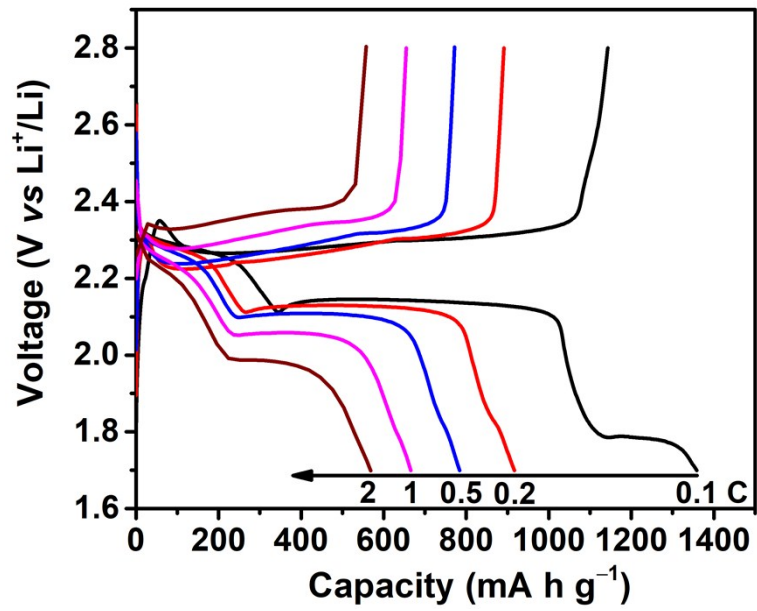


Fig. S12 Discharge/charge profiles of yolk-shell NiS₂/C-S cathode tested at various current densities.

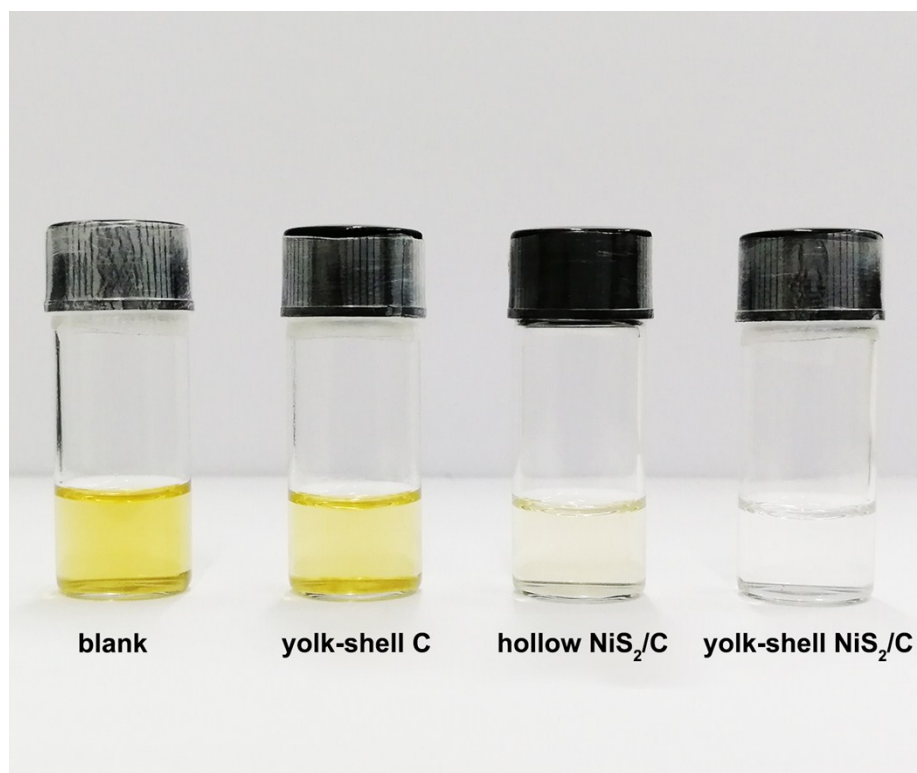


Fig. S13 Visualized adsorption of Li_2S_6 with yolk-shell C, hollow NiS_2/C , and yolk-shell NiS_2/C .

Table S1. Electrochemical performance comparison of yolk-shell NiS₂/C-S cathode with reported sulfur cathodes for Li-S batteries.

Sample	Sulfur content (wt%)	Rate performance		Cycling performance	Ref.
		Capacity (mA h g ⁻¹)	Current density		
Yolk-shell NiS₂/C-S	70	1358, 917, 784, 666, and 569	0.1, 0.2, 0.5, 1, and 2 C	394 mA h g⁻¹ after 200 cycles at 1 C	This work
TiN-S	59	1121, 899, 776	0.1, 0.5, and 1 C	644 mA h g ⁻¹ after 500 cycles at 0.5 C	S2
NiS ₂ /C-S	56	1203, 941, 788, 702, and 574	0.1, 0.2, 0.5, 1, and 2 C	730 mA h g ⁻¹ after 200 cycles at 0.5 C	S3
Co-N-doped C-S	64	1303, 1147, 994, and 694	0.1, 0.2, 0.5, and 1 C	669 mA h g ⁻¹ after 600 cycles at 1 C	S4
CeO ₂ @CNT-S	60	1359, 1033, 868, and 715	0.1, 0.2, 0.5, and 1 C	173 mA h g ⁻¹ after 600 cycles at 0.5 C	S5
TiO ₂ /rGO-S	60	1285, 984, 898, and 803	0.1, 0.2, 0.5, and 1 C	631 mA h g ⁻¹ after 200 cycles at 0.5 C	S6
Co ₃ S ₄ /CNT-S	70	1330, 1165, 988, 859, and 702	0.2, 0.5, 1, 2, and 5 C	752 mA h g ⁻¹ after 500 cycles at 1C	S7
MnO ₂ @Hollow carbon fibers-S	71	1161, 1090, 1010, 890, and 690	0.05, 0.1, 0.2, 0.5, and 1 C	662 mA h g ⁻¹ after 300 cycles at 1C	S8
TiO@C-S	70	1146, 1029, 910, 800, and 655	0.1, 0.2, 0.5, 1, and 2 C	630 mA h g ⁻¹ after 500 cycles at 0.5 C	S9
VS ₂ /rGO-S	64	1133, 987, 875, 616, and 401	0.5, 1, 2, 3, and 5 C	662 mA h g ⁻¹ after 1200 cycles at 1 C	S10
VN/Graphene-S	56	1447, 1241, 1131, 953, and 710	0.2, 0.5, 1, 2, and 3 C	1128 mA h g ⁻¹ after 200 cycles at 1 C	S11

References

- S1 F. Zou, Y. M. Chen, K. Liu, Z. Yu, W. Liang, S. M. Bhaway, M. Gao and Y. Zhu, *ACS Nano*, 2016, **10**, 377.
- S2 Z. M. Cui, C. X. Zu, W. D. Zhou, A. Manthiram and J. B. Goodenough, *Adv. Energy Mater.*, 2016, **28**, 6926.
- S3 Y. Lu, X. N. Li, J. W. Liang, L. Hu, Y. C. Zhu and Y. T. Qian, *Nanoscale*, 2016, **8**, 17616.
- S4 M. E. Zhong, J. D. Guan, Q. J. Feng, X. W. Wu, Z. B. Xiao, W. Zhang, S. Tong, N. Zhou and D. X. Gong, *Carbon*, 2018, **128**, 86.
- S5 D. J. Xiao, C. X. Lu, C. M. Chen and S. X. Yuan, *Energy Storage Mater.*, 2018, **10**, 216.
- S6 J. H. Song, J. M. Zheng, S. Feng, C. Z. Zhu, S. F. Fu, W. G. Zhao, D. Du and Y. H. Lin, *Carbon*, 2018, **128**, 63.
- S7 T. Chen, Z. W. Zhang, B. R. Cheng, R. P. Chen, Y. Hu, L. B. Ma, G. Y. Zhu, J. Liu and Z. Jin, *J. Am. Chem. Soc.*, 2017, **139**, 12710.
- S8 Z. Li, J. T. Zhang and X. W. Lou, *Angew. Chem. Int. Ed.*, 2015, **54**, 12886.
- S9 Z. Li, J. Zhang, B. Guan, D. Wang, L. M. Liu and X. W. Lou, *Nat. Commun.*, 2016, **7**, 13065.
- S10 Z. B. Cheng, Z. B. Xiao, H. Pan, S. Q. Wang and R. H. Wang, *Adv. Energy Mater.*, 2018, **8**, 1702337.
- S11 Z. H. Sun, J. Q. Zhang, L. C. Yin, G. J. Hu, R. P. Fang, H. M. Cheng and F. Li, *Nat. Commun.*, 2017, **8**, 14627.